Proc. of IEEE ISPLC 2014, Glasgow, May 2014

A G3-PLC Simulator for Access Networks

Luca Di Bert*, Salvatore D'Alessandro*, Andrea M. Tonello*†
*WiPLi Lab - Università di Udine - Via delle Scienze 208 - 33100 Udine - Italy
†WiTiKee s.r.l. - Via Duchi D'Aosta 2 - 33100 Udine - Italy
e-mail: luca.dibert@uniud.it, salvatore.dalessandro@uniud.it, tonello@uniud.it

***Abstract*—The paper proposes a cross-platform simulator that allows to realistically simulate G3-PLC systems up to the network layer. The platform consists of two simulators: one for the physical (PHY) layer and one for the data link (DLL)/adaptation (ADP) layer. The former is implemented in MATLAB, while the latter in OMNeT++. To improve the performance and coverage of G3-PLC, a simple adaptive tone mapping algorithm together with a routing algorithm are also presented. The performance of G3-PLC is presented considering different smart grid (SG) applications in the access network scenario, although the simulation platform can be also used in the context of home networks.**

I. Introduction

The smart grid (SG) can be seen as a communications network that needs to deliver flows of data to offer several services over different domains [1]: *generation*, *transmission*, *distribution*, and *customer*. Some examples of services are: automatic meter reading (AMR), meter events and alarms, substations automation, microgrids integration, demand response through the smart management and monitoring of household appliances, control of local renewable energy plants, integration of plug-in electric vehicles, etc.. To offer this plethora of services, it is fundamental to adopt/develop adequate communication technologies capable of satisfying the communication requirements of each service, e.g., throughput, frame error rate (FER), end-to-end delay, etc..

Although finding the best communication technology for SG applications is not straightforward, recently, industries and standardization organizations have proposed the use of narrow band (NB) power line communication (PLC) as a cost-effective solution to support the development of the SG concept. Several solutions and standards have been conceived and developed for this scope. Among them, G3-PLC [2] is playing a significant role inasmuch it has been used as the basis for the development of the IEEE P1901.2 [3] standard and the ITU-T G.hnem [4] standard for SG applications. In this context, it is important to have a simulation tool that permits to predict the performance of such a technology in different scenarios.

In this paper, we present a cross-platform simulator that allows for simulating the G3-PLC technology. We consider the distribution domain as application scenario, and in particular the access network.

Although several network simulators are nowadays available, e.g., ns-2, ns-3, OMNeT++, JiST and SimPy, a comprehensive implementation and simulation of a G3-PLC system has not been performed yet. This is because of the implementation issues related to physical (PHY) layer modeling within a network simulator, which has not been thought for these purposes. In fact, PHY modeling exploits signal processing techniques whose integration in network simulators is rather costly from a computational point of view. Furthermore, the computational complexity grows with the number of considered communication technologies and network devices. On the other hand, network simulators are well suited for higher layers simulation, e.g., medium access control (MAC) algorithms, network procedures and transport protocols, and are optimized for these purposes [5].

The proposed cross-platform consists of two different simulators: one for the physical (PHY) layer and one for the data link layer (DLL)/adaptation (ADP) layer. The PHY layer simulator is implemented in MATLAB and it is used to compute the channel responses of the links in a given network. Furthermore, it computes two PHY layer performance metrics: the frame error rate (FER) and the the bit-rate of each link. These two metrics are used to abstract the PHY layer within the DLL/ADP layer simulator, which is implemented in OMNeT++. In order to improve the G3-PLC performance, the PHY layer simulator implements a simple bit loading algorithm that aims at maximizing the bit-rate under a power and a bit-error-rate (BER) constraint. The DLL/ADP layer simulator implements the MAC sub-layer and a routing algorithm that determines the best routing path based on a metric that uses the information provided by the PHY layer.

The remainder of the paper is as follows. Sections II and III respectively describe the PHY and the DLL/ADP simulators. Numerical results are reported in Section IV. Finally, the conclusions follow in Section V.

II. PHY Layer Simulator

The PHY layer Simulator is composed by a network topology simulator and a G3-PLC simulator. These are respectively described in the following Sections II-A and II-B.

A. Network Topology Simulator

We consider the application of G3-PLC in the low voltage (LV) power distribution grid, and in particular between the medium voltage (MV)/LV transformer stations and the house meters, i.e., in the access network [6, §2.3].

A general description of the characteristics of the EU access network topology can be found in [6], [7], [8]. Beside the previous works, [9] proposes a topology model that is mainly developed for US grids. According to the previous works, there are differences between European and US/Asia

networks. However, in general, there is an agreement on the characteristics of the network topologies. Regarding the EU network, which will be considered from now on, it is agreed that from the MV-LV transformer a three phase backbone starts. Then, from the backbone one or more branches (up to 10) can be present where tens of households per branch can be connected (see [8, §3], [6, §3], [7, §2]). The network length, namely the maximum distance between the MV-LV transformer and the households, is up to 1 Km, while the number of houses that are fed by a given MV/LV transformer station varies between some tens to one/two hundreds. In US the density of the houses is smaller than in EU with a consequent increase in the number of MV-LV transformers. Furthermore, the maximum network length is much smaller (hundreds of meters).

In order to simulate an access network, we made use of the bottom-up channel generator presented in [10]. Briefly, this simulator generates the channels frequency response between pairs of network nodes from the physical description of the network, namely from knowledge of the topology, cables and loads. We consider NAYY150SE cables for the backbone and the branches (150 mm^2 area for each of the four cores), and NAYY50SE cables to connect the household to the branches (50 mm^2 area of each of the 2 cores). The last important parameter to consider is the access impedance, i.e., the impedance seen at the house connection box. To this respect, we highlight that the literature is really poor, and we only found the work of Sigle [11] that reports three examples of measured access impedance up to 500 kHz. Among these examples, we used the two access impedances measured in households of a residential scenario to model the households in our network.

Fig. 1 shows an example of access network topology, it will be used in this work to obtain numerical results. It represents a residential area of about 92,000 m^2 where 25 houses connected to 7 branches are fed by a single MV/LV transformer. Each house is identified by a number between 13 and 58, and the MV/LV transformer station is identified by the number 1. For the considered topology, 650 channel frequency responses within 30–500 kHz have been generated. Some examples are reported in Fig. 2.

Regarding the noise, we model it according to [12] and [13] as a Gaussian background noise in the NB (3-500 kHz). In particular, we assume the PSD of the noise to decrease exponentially as it is shown in Fig. 2.

B. G3-PLC Simulator

According to [14], G3-PLC technology has been designed to support CENELEC bands (3–148.5 kHz) and FCC band (9–490 kHz). In detail, CENELEC specifies four frequency bands: the band A (3–95 kHz) is reserved to power utilities, the band B (95–125 kHz) can be used for any application, the band C (125–140 kHz) is dedicated to in-home networking systems, the band D (140–148.5 kHz) is reserved to alarm and security systems. G3-PLC is able to work in a combination of two or more CENELEC bands, i.e., BC, BCD and BD.

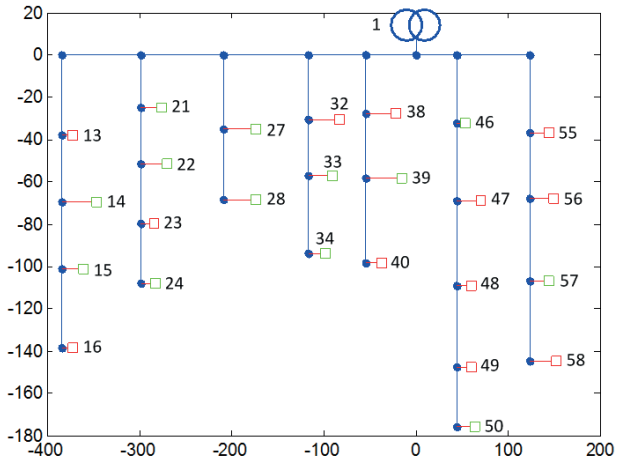

Fig. 1: Physical network topology and host ID.

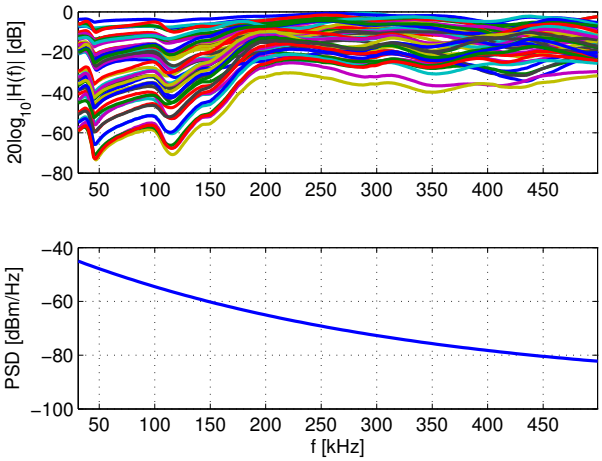

Fig. 2: Top: examples of channel frequency response realizations for the network shown in Fig. 1. Bottom: PSD profile of the background noise.

According to [2], G3-PLC adopts pulse shaped orthogonal frequency division multiplexing (PS-OFDM) modulation combined with a differential binary phase shift keying (DBPSK) or differential quadrature phase shift keying (DQPSK) schemes where the phases of carriers in the adjacent symbol are taken as reference for detecting the phases of the carriers in the current symbol. Two different transmission modes are allowed, namely, *normal* and *robust*. In normal mode, forward error correction (FEC) encoding (thus decoding) is composed of a Reed-Solomon (RS) and a convolutional encoder, while, in robust mode, beside RS and convolutional encoding, there is a repetition code (RC) that repeats each bit following the preamble 4 times, making the system more robust to channel impairments. It is worth noting that DBPSK can be adopted in both normal and robust modes, while DQPSK only in normal mode.

Since we are interested in SG applications in the LV distribution grid, when showing numerical results, we consider G3-PLC working in CENELEC A and FCC bands. The

corresponding PHY layer parameters are listed in TABLE I. We also assume that each PHY frame is composed of 20 and 56 PS-OFDM symbols, respectively for CENELEC A and FCC, each carrying data modulated with robust DBPSK. This assumption respectively leads to 22 and 12 bytes of payload dimension. Consequently, the maximum achievable bit-rates is 3.26 $kbps$ and 10.17 $kbps$ for CENELEC A and FCC band, respectively. TABLE II reports other reference PHY layer parameters that will be used for the simulations. A detailed set of PHY layer parameters for G3-PLC can be found in [4].

TABLE I: G3-PLC system parameters.

	CENELEC A	FCC
Number of IFFT/FFT points (M)	256	256
Number of modulated carriers (N_c)	36	72
First modulated carrier frequency (f_1) [kHz]	35.938	145.3
Last modulated carrier frequency (f_2) [kHz]	90.625	478.125
Available bandwidth ($f_2 - f_1$) [kHz]	54.688	342.2
Sampling frequency (f_s) [MHz]	0.4	1.2
Frequency spacing (f_s/M) [Hz]	1562.5	4687.5
Number of overlapped samples (N_o)	8	8
Number of cyclic prefix samples (N_{CP})	30	30
Number of FCH symbols (N_{FCH})	13	12
Number of preamble symbols (N_{pre})	9.5	9.5
Preamble duration [ms]	6.08	2.0267
PS-OFDM symbol duration [μs]	695	231.7

TABLE II: G3-PLC simulation parameters.

	CENELEC A	FCC
Transmitted PSD [dBm/Hz]	-13	
Carrier modulation	robust DBPSK	robust DBPSK
Number of PS-OFDM symbols per PHY frame (N_s)	56	20
PHY frame duration [ms]	54	9.4
PHY payload dimension n [bytes]	22	12
Maximum PHY data rate [kbps]	3.26	10.17

1) Adaptive Tone Mapping: G3-PLC permits the use of bit and power loading algorithms. According to [2], the transmitter performs a tone map request exploiting the frame control header (FCH), which is a multi symbol field following the preamble. Upon reception of a tone map request, the receiver estimates the signal-to-noise ratio (SNR) of the received signal for each modulated carrier, and informs the remote transmitter with a tone map response. At this point, the transmitter is able to adaptively select the usable tones, optimum modulation and code rate to ensure a reliable communication. In particular, the transmitter selects the tones where to send data symbols, and the ones where to send dummy data symbols (noise) that have to be discarded at the receiver. It is important to note that the choice of the loading algorithm to be implemented is up to the chip maker.

To this respect, we propose to use a very simple on-off loading algorithm. The proposed bit-loading algorithm targets the bit rate maximization under a BER and a power constraint on each carrier, and a constraint on the constellation to be employed. It can be formulated as follows

$$\max \quad R = \sum_{k \in \mathbb{N}_C} b^{(k)}, \tag{1}$$

$$\text{s.t.} \quad BER^{(k)} \leq \gamma, \tag{2}$$

$$b^{(k)} \in \{0, 1\}, \quad P^{(k)} \leq \bar{P}, \quad \forall k \in \mathbb{N}_C \tag{3}$$

where $b^{(k)}$, $BER^{(k)}$, $P^{(k)}$, and $\bar{P}$ respectively represent the bits loaded, the bit error rate (BER) and the transmitted power on carrier k, and the maximum transmit power on each carrier, which is assumed to be constant, e.g., it is given by a power spectral density (PSD) mask constraint. Furthermore, $\mathbb{N}_C$ denotes the set of modulated carriers. It is well known that for uncoded systems the BER constraint is equivalent to an SNR constraint [15]. Furthermore, an SNR gap can be considered for a given channel coding scheme [15]. In our case, we decided to choose the SNR gap, or equally the SNR threshold, from the curves of the average BER (averaged across carriers) obtained for uncoded and coded DBPSK (see Fig. 3). In particular, we set the SNR threshold equal to 2 dB, so that the BER of the coded system is of about 10^{-4}. Fig. 3 has been obtained using the G3-PLC system in CENELEC A band with the parameters of Tables I, and II, and the noise shown in Fig. 2. We notice that although not shown, similar results have been obtained for the FCC band. Furthermore, in Fig. 3, the curve labeled with "theoretical" shows the theoretical BER for the uncoded DBPSK system, computed as described in [16, § 5].

Now, once the SNR threshold is set, problem (1) is solved by loading DBPSK symbols only in those carriers whose SNR is higher or equal to the threshold. As it will be shown in the numerical results section, the proposed bit-loading algorithm allows for satisfying the BER constraint.

The simulation of the described PHY layer is carried out in MATLAB and it is meant to compute the bit-rate and the FER of each link. These two parameters are then used by the DLL/ADP simulator to abstract the PHY layer. We notice that although in this work the two simulators are disjoint, they could be connected by developing the Matlab routines in C/C++ to run in OMNeT++.

III. DLL and ADP Layer Simulator

The DLL and ADP layer simulator is implemented using OMNeT++ which is an event based simulator that allows for implementing channel access policies, routing algorithms and traffic models.

The DLL simulation essentially corresponds to the implementation of the MAC sub-layer. In this respect, the MAC sub-layer of G3-PLC is based on the IEEE 802.15.4–2006 specifications for low-rate wireless personal area networks (WPANs) [17]. Basically, the channel access method is based on carrier sense multiple access with collision avoidance (CSMA/CA) mechanism and a random backoff time. Details can be found in [18].

Beside the MAC sub-layer, G3-PLC specifies an adaptation (ADP) layer which is based on the IPv6 over Low power Wireless Personal Area Networks (6LoWPAN) [19]. Furthermore,

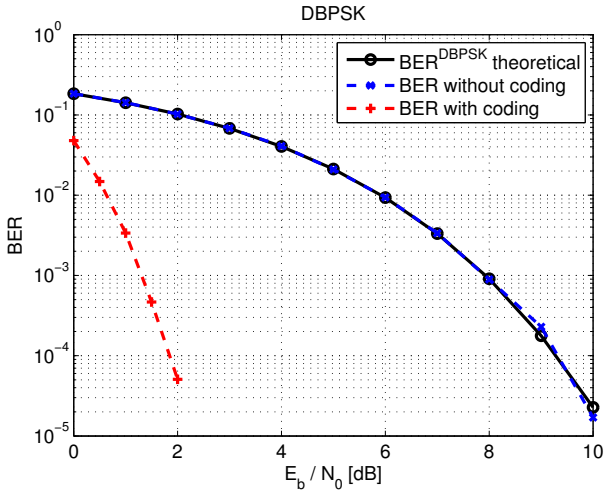

Fig. 3: BER vs E_b/N_0 for DBPSK modulation with and without coding.

6LoWPAN Ad hoc Routing Protocol (LOAD) [20], which is a simplified form of AODV for 6LoWPAN, is selected as an effective routing protocol to handle changing link conditions. LOAD operates on ADP layer creating a logical network topology below the IPv6 network layer. For the IPv6 layer, the 6LoWPAN adaptation layer is considered as a single link. LOAD is designed to find the optimized route that minimizes the route cost (RC) as follows

$$\min_i \left\{ \mathrm{RC}\left(p^{(i)}\right) \right\}, \tag{4}$$

where p_i denotes the i-th route from the source to the destination. Since the standard does not specify the metric for the route cost, we propose to define it as follows

$$\mathrm{RC}\left(p^{(i)}\right) = -\frac{1}{N_H^{(i)}} \prod_{h=0}^{N_H^{(i)}-1} C\left\{[D_h, D_{h+1}]\right\}, \tag{5}$$

where the i-th route goes through the nodes $D_0, D_1, \ldots, D_{N_H^{(i)}}$. $N_H^{(i)}$ denotes the number of hops ($0 < N_H^{(i)} \leq \mathrm{adpMaxHops}$), and $C\left\{[D_x, D_y]\right\}$ is the link cost between device D_x and D_y. We notice that, according to [18], we consider $\mathrm{adpMaxHops} = 4$. As regards the link cost, we propose to take into account PHY transmission parameters and to model it as follows

$$C\left\{[D_x, D_y]\right\} = \left(1 - FER\left\{[D_x, D_y]\right\}\right) \frac{N_c^{ON}\left\{[D_x, D_y]\right\}}{N_c}, \tag{6}$$

where $FER\left\{[D_x, D_y]\right\}$ is the FER associated to the link between nodes D_x and D_y. $N_c^{ON}\left\{[D_x, D_y]\right\}$ is the number of *on* carriers (see Section II-B1), and N_c the total number of modulated carriers. It is worth noting that the proposed link cost corresponds to the probability of receiving correct bits. Furthermore, the route cost takes into account the delay of the route with the term $1/N_H^{(i)}$ (by assuming the delay of each link to be constant).

Now, in order to evaluate the G3-PLC performances, we consider two representative metrics, i.e., the throughput and the average end-to-end delay of each node. The throughput is computed as

$$THR^{(u)} = 8n\hat{N}_{RX}^{(u)} \quad [bps], \tag{7}$$

where n is the PHY payload dimension in bytes per transmitted frame and $\hat{N}_{RX}^{(u)}$ is the number of correct received PHY frames per second send by the u-th node to the coordinator.

The average end-to-end delay is computed as the time lapse between the instant when a frame is sent from the source and the instant when the frame is received at the destination. It is computed as follows

$$t_{e2e}^{(u)} = \frac{1}{N_{RX}^{(u)}} \sum_{i=1}^{N_{RX}^{(u)}} N_H^{(i)} \left(t_q^{(i)} + t_{tx}^{(i)} + t_p^{(i)} \right), \tag{8}$$

where $N_{RX}^{(u)}$ is the total number of correct frames received by the coordinator and sent by the u-th node. Moreover, queuing ($t_q^{(i)}$), transmission ($t_{tx}^{(i)}$) and propagation ($t_p^{(i)}$) delays for the i-th frame are weighted for the factor $N_H^{(i)}$, which is number of hops ($N_H^{(i)} > 0$) the frame has to do in order to reach the destination. We notice that processing delays at the transmitter and receiver have been assumed ideal. Furthermore, since the propagation delay in electric cables is 5.775 $\mu s/km$ [2], we neglect its contribution.

A. Network Traffic

In order to simulate the behavior of G3-PLC in the access network, we need to model the traffic that is required by the SG applications. To this end, we consider the work [21] according to which SG applications generate traffic that can be classified into three categories: mission-critical, soft real-time, and non-real-time traffic profiles. Mission-critical traffic represents alarm-response commands and it is classified into LOW-LOW (3 ms), LOW (16 ms), MEDIUM (160 ms), and HIGH ($>$ 160 ms) latency classes [22]. Soft real-time traffic regards interactive maintenance commands, periodic meter readings and other sensor measurements. In this case, commands and measurements are sporadic (with periods in the order of 1–15 min [23]), and latency requirements are soft ($\sim$ 1 min). Finally, non-real-time traffic profile refers to the planning of services to exchange information, e.g, firmware updates and file-transfer operations. It requires higher information rates than the previous traffics, but it is delay-tolerant.

The previous traffic categories provide a description of SG application requirements, but they are not sufficient for testing network performances. To this aim, according to [21], we consider the traffic generated by energy services interfaces (ESIs), i.e., network nodes, to be directed to the distribution access point (DAP), i.e., the MV/LV transformer station. In TABLE III, we detail the considered traffic models.

IV. Numerical Results

In order to show the functionality of the proposed cross-platform simulator, we consider the network of Fig. 1 where we assume the communication to be from the network nodes 13–53 to the network coordinator (node 1).

TABLE III: Smart Grid traffic model.

Traffic description	Traffic generation	Mean value [s]	Packets / dimension [bytes]
Alarm signals	Exponential	240	1 / 1000
Network joining	Exponential	3600	1 / 1000
Metering data	Exponential	60	1 / 1000
Telemetry signals	Exponential	60	1 / 1000
Information reports	Exponential on-off traffic	$T_{on} = 0.2$ $T_{off} = 10$	–

The first scenario that we consider consists of the transmission of 10^4 frames from each node to the coordinator. It is meant to show the functionality of adaptive tone mapping (see Section II-B1). Fig. 4 shows the BER, the FER, and the throughput for the considered scenario with and without the use of tone mapping, when no relay is used, namely when the communication exploits the direct link between transmitter and receiver. The considered frequency band is the CENELEC A. Regarding the FCC band, we report that in the considered topology, almost all nodes achieve the maximum PHY data rate, i.e., 10.17 *kbps* (see TABLE II). From Fig. 4, we can see that the use of tone mapping decreases the BER to the expected value of about 10^{-4} and in some cases also increases the throughput, e.g., node ID 21 and 22. Furthermore, it is worth noting that nodes 13, 14, 15, 16, 23 and 24 are not visible from the coordinator since their correspondent throughput is 0. We highlight that this behavior is due to the fact that none of these node experience in their modulated carriers an SNR that is higher than the threshold, therefore they do not transmit data at all (see Section II-B1).

A. MAC/ADP Layer Simulation

The second scenario that we consider is the following. We assume a metering scenario. In detail, a smart meter, represented by a G3-PLC node, is placed in every house and it transmits 1 frame of data per power measurement to the coordinator. In this perspective, according to the worst case in [24], we assume that each node generates traffic according to an exponential distribution with mean equal to 60 s.

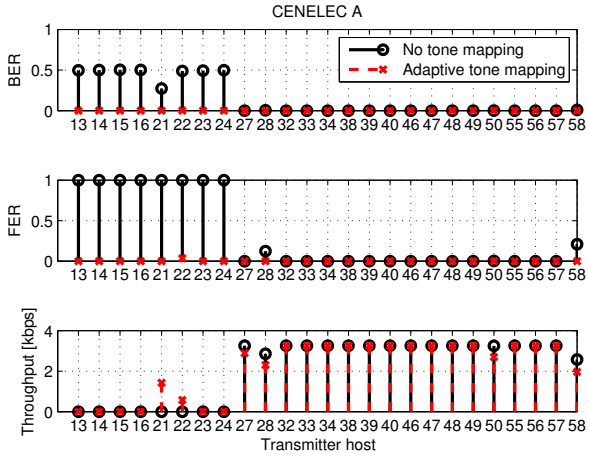

Fig. 4: BER, FER, and throughput for direct link communication between each network node and the coordinator.

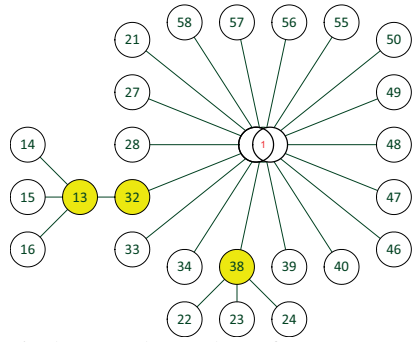

Fig. 5: Logical network topology for CENELEC A band.

Fig. 5 shows the logical network topology as the result of the application of the routing algorithm for CENELEC A band. It is worth noting that few nodes (yellow circles) act as relay, in order to allow the communication between all network nodes and coordinator. Regarding the FCC band, we notice that with the considered network topology, no relay turns out to be used. However, this behavior may not be true in general. Fig. 6 reports the throughput and the end-to-end delay for both frequency bands. Furthermore, regarding CENELEC A, the results are reported either for the case when the routing algorithm (LOAD) is adopted or when it is not. It is interesting to note that, when LOAD is applied, all network nodes reach almost the same throughput (this is because the network is overloaded) and the network coverage is improved. However, the delays of relayed frames are proportional to the number of hops, according to Eq. 8. As last scenario, we consider the case where different SG applications run over the network. From TABLE III, we notice that, alarm signals, network joining, metering data and telemetry signals are characterized by a single packet of 1000 bytes. However, there is no configuration of G3-PLC parameters which supports a single PHY frame with a dimension of 1000 bytes. Therefore, to cope with this problem, we consider two cases: (i) the transmission of a single frame with maximum dimension of

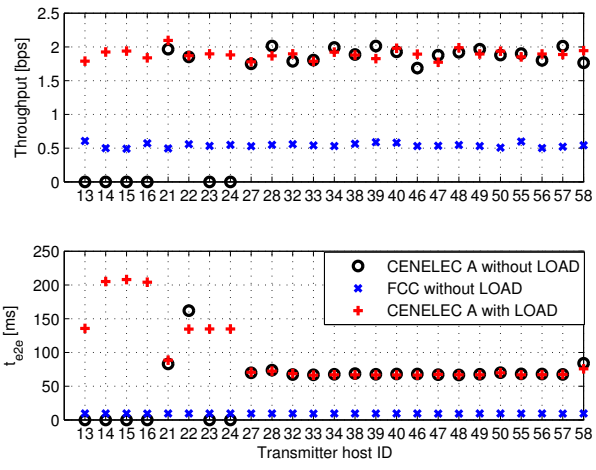

Fig. 6: Throughput and end-to-end delay for metering traffic.

22 and 12 bytes, respectively for CENELEC A and FCC, and (ii) the transmission of a frame burst whose total dimension is 1000 bytes. The traffic model has been applied so that every network node transmits to the coordinator. A total of 6 hours of simulations have been performed. Fig. 7 shows

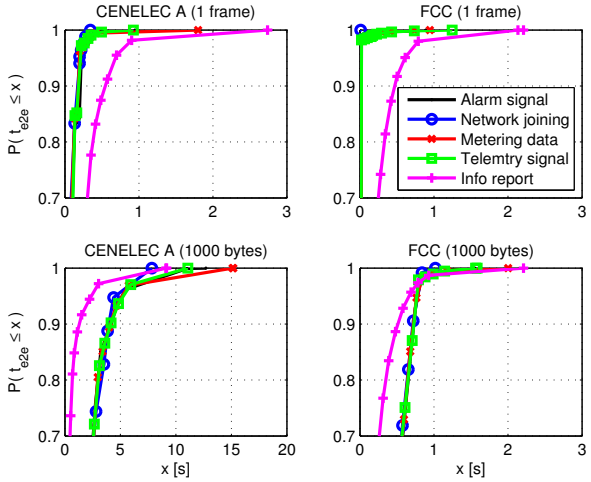

Fig. 7: CDF of the end-to-end delay for different traffic profiles in CENELEC A and FCC bands.

the cumulative distribution function (CDF) of the end-to-end delay of each traffic profile. In particular, top-left and top-right figures show the CDF for a single frame transmission, respectively for CENELEC A and FCC bands. Bottom-left and bottom-right figures show the CDF for a frame burst of 1000 bytes, respectively for CENELEC A and FCC bands. From Fig. 7 one can assert whether or not a given class of service can be offered. As an example, we can assert that LOW (16 ms) and MEDIUM (<160 ms) latency class services of alarm-response command cannot be offered in both CENELEC A or FCC bands assuming 1000 bytes of data in the considered network topology and with the considered G3-PLC system parameters.

V. Conclusion

A cross-platform simulator for G3-PLC has been presented. The PHY layer is implemented in Matlab and consists of a network topology and a transmission system simulator. The bit-rate and the frame error rate of each link are used to abstract the PHY layer in the DLL/ADP layer simulator that is implemented in OMNeT++. The presented simulator gives the possibility to predict the behavior of G3-PLC over a given application scenario and to see whether the constraints of a given service are satisfied or not. From simulation results over an access network, it has been found that adaptive bit-loading together with routing algorithms are needed to improve the network coverage and throughput of G3-PLC especially when working in CENELEC-A frequency band.

References

[1] National Institute of Standards and Technology, *NIST Framework and Roadmap for Smart Grid Interoperability Standards, Release 1.0*, Office of the National Coordinator for Smart Grid Interoperability, U.S. Department of Commerce, Jan. 2010.

[2] ERDF, *PLC G3 Physical Layer Specification*. [Online]. Available: http://www.maxim-ic.com/products/powerline/pdfs/G3-PLC-Physical-Layer-Specification.pdf

[3] O. Logvinov, *Netricity PLC and the IEEE P1901.2 Standard*, HomePlug Powerline Alliance.

[4] ITU-T G.9903, *Narrowband orthogonal frequency division multiplexing power line communication transceivers for G3-PLC networks*, Oct. 2012.

[5] E. Weingartner, H. vom Lehn, and K. Wehrle, "A Performance Comparison of Recent Network Simulators," in *Communications, 2009. ICC '09. IEEE International Conference on*, 2009, pp. 1–5.

[6] H. C. Ferreira, L. Lampe, J. Newbury, and T. G. Swart, *Power Line Communications: Theory and Applications for Narrowband and Broadband Communications over Power Lines*. NY: Wiley & Sons, 2010.

[7] Opera Consortium, "Deliverable D4: Theoretical postulation of PLC channel model," Tech. Rep., 2005.

[8] H. Hrasnica, A. Haidine, and R. Lehnert, *Broadband Powerline Communications: Network Design*. Wiley, 2004.

[9] Z. Wang, A. Scaglione, and R. J. Thomas, "Generating Statistically Correct Random Topologies for Testing Smart Grid Communication and Control Networks," *IEEE Trans. On Smart Grid*, vol. 1, no. 1, Jun. 2010.

[10] A. Tonello and F. Versolatto, "Bottom-Up Statistical PLC Channel Modeling – Part II: Inferring the Statistics," *Power Delivery, IEEE Transactions on*, vol. 25, no. 4, pp. 2356–2363, 2010.

[11] M. Sigle, W. Liu, and K. Dostert, "On the impedance of the low-voltage distribution grid at frequencies up to 500 kHz," in *Proc. of Int. Symp. on Power Line Commun. and Its App. (ISPLC)*, Bejing, China, March 2012, pp. 30–34.

[12] T. Zheng, X. Yang, B. Zhang, and et al., "Statistical analysis and modeling of noise on 10-kv medium-voltage power lines," *IEEE Transactions on Power Delivery*, vol. 22, no. 3, pp. 1433–1439, Jul. 2007.

[13] K. Razazian, A. Kamalizad, M. Umari, Q. Qu, V. Loginov, and M. Navid, "G3-plc field trials in u.s. distribution grid: Initial results and requirements," in *Proc. of Int. Symp. on Power Line Commun. and Its App. (ISPLC)*, April 2011, pp. 153–158.

[14] ITU-T G.9901, *Narrowband orthogonal frequency division multiplexing power line communication transceivers – Power spectral density specification*, Nov. 2012.

[15] N. Papandreou and T. Antonakopoulos, "Bit and Power Allocation in Constrained Multi-carrier Systems: The Single-User Case," *EURASIP J. on Advances in Signal Processing*, vol. 2008, no. Article ID 643081, 2008.

[16] J. Proakis, *Digital Communications*, ser. McGraw-Hill series in electrical and computer engineering. McGraw-Hill Higher Education, 2001.

[17] *IEEE Std 802.15.4-2006, Part 15.4: Wireless Medium Access Control (MAC) and Physical Layer (PHY) Specifications for Low-Rate Wireless Personal Area Networks (WPANs)*, IEEE, 2006.

[18] ERDF, *PLC G3 MAC Layer Specification*. [Online]. Available: http://www.maxim-ic.com/products/powerline/pdfs/G3-PLC-MAC-Layer-Specification.pdf

[19] N. Kushalnagar, G. Montenegro, and C. Schumacher, *IPv6 over Low-Power Wireless Personal Area Networks (6LoWPANs): Overview, Assumptions, Problem Statement, and Goals*, Internet Engineering Task Force (IETF), 2007.

[20] K. Kim, S. D. Park, G. Montenegro, S. Yoo, and N. Kushalnagar, *6LoWPAN Ad Hoc On-Demand Distance Vector Routing (LOAD)*, Internet Engineering Task Force (IETF), 2007.

[21] F. Gomez-Cuba, R. Asorey-Cacheda, and F. Gonzalez-Castano, "Smart Grid Last-Mile Communications Model and Its Application to the Study of Leased Broadband Wired-Access," *Smart Grid, IEEE Transactions on*, vol. 4, no. 1, pp. 5–12, 2013.

[22] IEEE Standards Association, "IEEE Guide for Smart Grid Interoperability of Energy Technology and Information Technology Operation with the Electric Power System (EPS), End-Use Applications, and Loads," *IEEE Std 2030-2011*, pp. 1–126, 2011.

[23] M. Bauer, W. Plappert, C. Wang, and K. Dostert, "Packet-oriented communication protocols for Smart Grid Services over low-speed PLC," in *Proc. of IEEE Int. Symp. on Power Line Commun. and its App. (ISPLC)*, Dresden, Germany, 2009.

[24] D. Niyato, L. Xiao, and P. Wang, "Machine-to-machine communications for home energy management system in smart grid," *Communications Magazine, IEEE*, vol. 49, no. 4, pp. 53–59, 2011.